PROCEEDINGS OF SPIE

SPIEDigitalLibrary.org/conference-proceedings-of-spie

Micromachined water-immersible scanning mirror with torsional and bending hinges

Suangliang Li, Xiaoyu Duan, Jun Zou

Suangliang Li, Xiaoyu Duan, Jun Zou, "Micromachined water-immersible scanning mirror with torsional and bending hinges," Proc. SPIE 12013, MOEMS and Miniaturized Systems XXI, 120130C (1 March 2022); doi: 10.1117/12.2608892

SPIE.

Event: SPIE OPTO, 2022, San Francisco, California, United States

Micromachined water-immersible scanning mirror with torsional and bending hinges

Shuangliang Li, Xiaoyu Duan and Jun Zou

Department of Electrical and Computer Engineering, Texas A&M University
College Station, TX USA 77843

Abstract

This paper reports a new two-axis water-immersible micro scanning mirror (WIMSM) using torsional and bending BoPET (biaxially-oriented polyethylene terephthalate) hinges. A micromachining-based fabrication process is developed to enable high patterning resolution and alignment accuracy and to reduce the amount of manual assembly. With a torsional hinge, the fast axis has a resonance frequency of ~300 Hz in air and ~200 Hz in water. With a bending hinge, the slow axis has a resonance frequency of 60~70 Hz in air and 20~40 Hz in water. 2D B-scan and 3D volumetric ultrasound microscopy are demonstrated by using the hybrid-hinge scanning mirror. The ability of scanning the slow axis at DC or very low frequencies allows a dense raster scanning pattern to be formed for improving both the imaging resolution and field of view.

Keywords: Water-immersible micro scanning mirror, torsional and bending hinges, ultrasound microscopy, photoacoustic microscopy

1. INTRODUCTION

Recently, MEMS (microelectromechanical systems) scanning mirrors have been developed to provide fast scanning of light beams in air for a number of optical applications, such as LiDAR (Light Detection and Ranging) [1, 2], variable optical attenuator (VOA) [3], fluorescence microscopy [4], optical endoscopy [5], etc. Further extending their applications in acoustic imaging, water-immersible micro scanning mirrors (WIMSMs) have been also investigated to steer focused optical and ultrasound beams under water (the most commonly used coupling medium for ultrasound propagation) [6-10]. Different from conventional MEMS scanning mirror designs (for operation in air), flexible polymer hinges are used in the WIMSMs to resist the possible shock damage in a liquid environment. In addition, the WIMSMs are usually driven by electromagnetic actuators, which do not require high voltages and can be easily made water-proof.

To achieve high imaging resolution, a dense 2D raster scanning pattern is desired, which requires the fast and slow axes to operate at two very different frequencies (e.g., 100s of Hz vs. several Hz). To obtain the maximal scanning range, the two scanning axes need to be driven at a frequency near their mechanical resonance. Therefore, the resonance frequencies of the fast and slow axes should be made different as much as possible. Previously, we investigated a new hybrid hinge design based on different deformation (torsional and bending) modes [11]. Specifically, the (stiffer) torsional hinge provides a high resonance frequency for the fast axis, while the (softer) bending hinge creates a low resonance frequency and enlarges the scanning range for the slow axis. By combing the torsional and bending modes, highly different driving frequencies of the fast and slow axes can be achieved with single (BoPET) hinge material. In this paper, we report a new miniaturized WIMSMs with both torsional and bending hinges. For demonstration, a prototype scanning mirror has been designed, fabricated and characterized. Its scanning performances was evaluated. Using the new scanning mirror, scanning ultrasound microscopy has also been conducted.

MOEMS and Miniaturized Systems XXI, edited by Hans Zappe, Wibool Piyawattanametha, Yong-Hwa Park, Proc. of SPIE Vol. 12013, 120130C · © 2022 SPIE
0277-786X · doi: 10.1117/12.2608892

2. DESIGN

Fig. 1 shows the schematic design of the micromachined water-immersible scanning mirror with torsional and bending hinges. The mirror plate is supported on the inner frame with two torsional hinges, which forms the fast axis. The inner frame is attached onto the outer frame with two bending hinges, which forms the slow axis. Two pairs of permanent magnets are bonded on the backside of the mirror plate. One pair of magnets is inversely magnetized to create a torque for actuating the fast axis (with two torsional hinges). The other pair has the same polarity to create a pushing or pulling force for actuating the slow axis (with two bending hinges). The entire mirror plate structure is fixed onto a 3D printed holder (with one or multiple inductor coils). A spacer structure is used to set the gap between the permanent magnets and the inductors coil(s) for the proper functioning of the scanning mirror. If the gap is too small, the attractive (magnetostatic) force between the core of inductor coil(s) and permanent magnets could become strong enough to pull-in the bending hinges and prevent the operation of the slow axis. However, a large gap will reduce the strength of the magnetic field from the inductor coil, resulting in higher driving currents and lower energy efficiency.

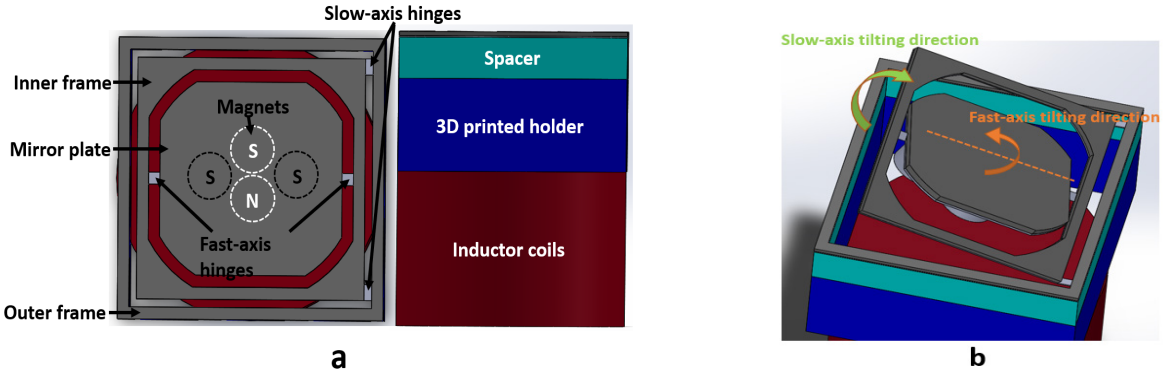

Fig. 1 (a) Schematic top and side views of the water-immersible scanning mirror with torsional and bending hinges. (b) Illustration of the deformation modes of the fast and slow axes (driven by single inductor coil).

For demonstration, a prototype scanning mirrors with an overall lateral dimension of $7 \times 7\ mm^2$ was designed, fabricated and characterized. Its main design parameters are listed in Tables 1. The scanning mirror is driven by four inductor coils connected in parallel. Their arrangement matches that of the four magnets on the mirror plate to maximize the driving efficiency. Because the fast and slow axes are supported by different torsion and bending hinges, their resonance frequencies vary significantly. As a result, their mechanical coupling will be well suppressed via the dynamic filtering effect [11]. To facilitate the design, the resonance frequencies (i.e., the eigenfrequencies) of the fast and slow axes in both air and water were simulated with COMSOL Multiphysics®. The resonance frequencies of the fast and slow axes in air are 307 Hz and 54 Hz, respectively. In water, they are reduced to 223 Hz and 39 Hz, respectively.

Table 1. Main design of parameters for the 7-by-7-mm mirror

7 by 7 mirror	Fast axis	Slow axis
Hinge size (l × w × t)	$0.3 \times 0.36 \times 0.07\ mm^3$	$0.2 \times 0.24 \times 0.07\ mm^3$
Rotational part (l × w)	$4.8 \times 4.8\ mm^2$	$6 \times 6\ mm^2$
Permanent magnets distance	1.6 mm	2.8 mm
The mirror size (l × w × t)	$7 \times 7 \times 0.2\ mm^3$	
Magnet's size (d × h)	$1.6 \times 0.8\ mm^2$	

3. FABRICATION AND ASSEMBLY

Fig. 2 shows the fabrication processes of the scanning mirror with torsional and bending hinges. Firstly, a 20-nm-thick chrome layer (as an adhesion promoter) was deposited on a 70-μm-thick BoPET film (Fig. 2a), which was bonded onto a 200-μm-thick silicon wafer (Fig. 2b). Secondly, a 20/200-nm-thick chrome/copper seed layer was deposited on the unbonded side of the BoPET film. A 600-nm-thick nickel layer was electroplated to serve as the etch mask for reactive ion etching of BoPET (Fig. 2c). Thirdly, a 300-nm aluminum layer was evaporated and patterned on the top side of silicon wafer to serve as the mask for cryogenic silicon etching [12] and also as the reflective layer of mirror plate (Fig. 2d). Next, four permanent magnet discs were attached underneath the fabricated mirror plate, which was bonded onto an acrylic spacer with epoxy (Fig. 2e). To complete the mirror assembly, four inductor coils were inserted into a 3D-printed holder, which was bonded with the spacer (Fig. 3).

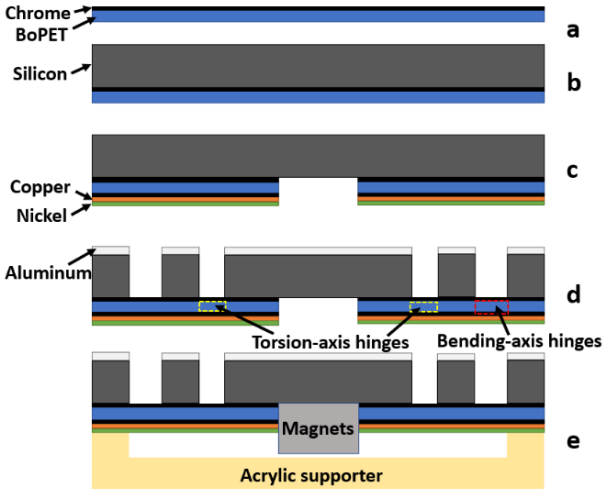

Fig. 2 Fabrication and assembly process flow of the mirror plate.

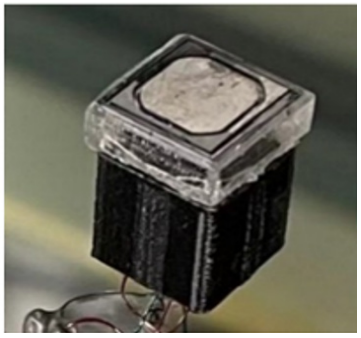

Fig. 3 Assembled prototypes of the scanning mirror。

4. CHARACTERIZATION

A laser tracing method was carried out to characterize the mirror scanning performance. The scanning mirror was fixed on a clamp at 45° downward. A collimated CW laser beam was incident horizontally onto the center of the mirror plate

and reflected onto a ruler at a certain distance. Based on the distance between the ruler and the laser point on the mirror surface and the length of the trace, the optical tilting angle of the mirror plate was calculated. Fig. 4 shows the tilting angles vs. frequency of the two axes in air and water, respectively. The resonance frequency is defined as the frequency where the maximum tilting angle was obtained. In air, the resonance frequencies of the fast and slow axes were determined as 311 Hz and 66 Hz, respectively. In water, the resonance frequencies were reduced to 206 Hz and 30 Hz, respectively. With bending hinges, significant increase in the viscous damping occurs on the slow axis in water, resulting in large reductions in its resonance frequency and quality factor, which makes it suitable for driving under DC or quasi-static conditions. During the testing, it was found out that the resonance frequencies of the two axes could drop slightly when the amplitude of the driving currents was increased. This phenomenon is due to the small openings on the mirror plate surface, which obstructs the air or water flow into and out of the fixture. When the mirror plate vibrates more under a larger current, it will subject to higher viscous damping, thereby reducing its resonance frequency. Therefore, for the characterization of the tilting angles with AC current driving, the driving frequencies were slightly adjusted to match the actual resonance frequencies at each current amplitude. In air, the resonance frequencies of the fast and slow axes were determined to be 311-322 Hz and 66-70 Hz, respectively. In water, the resonance frequencies were reduced to 205-216 Hz and 30-37 Hz, respectively.

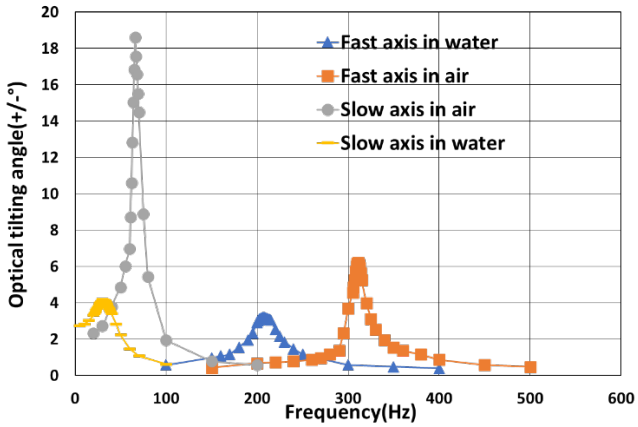

Fig. 4 Resonance frequency characterization of the fast and slow axes in the air and water for the scanning mirror. The amplitudes of the two AC driving currents (for the fast and slow axes) were 2.88 mA and 2.61 mA, respectively.

Fig. 5 shows the optical tilting angles at the adjusted resonance frequencies versus the AC driving current of the two axes in air and in water, respectively. Fig. 6 shows the tilting angle of the slow axis vs. the DC driving current in air and in water, respectively. At first, the optical tilting angles of the fast and slow axes increase almost linearly with the amplitude of the driving current, and more slowly at larger currents. This is because when the mirror plate is tilted to a larger angle, more misalignments will occur between the magnet and the inductor coil. Fig. 7 shows three representative laser scanning traces of the scanning mirror when the fast and slow axes were driven simultaneously by an AC and DC current, respectively. The AC current driving the fast axis was fixed at 3.3 mA at 206 Hz. The DC current of the slow axis was set to be -8.3 mA (-6.37º), 0 mA (0º) and 9.8 mA (5.54º), respectively. The tilting angle is slightly reduced at the two offset positions, which is mainly caused by the shifting of the resonance frequencies (from 206 Hz) at these two locations.

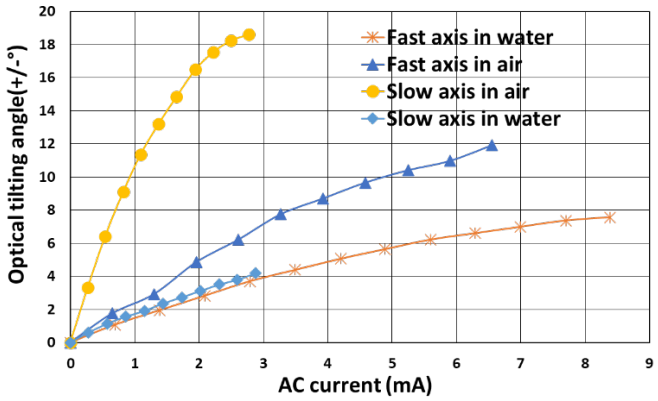

Fig. 5 Tilting angles of the fast and slow axes at the adjusted resonance frequencies for the scanning mirror.

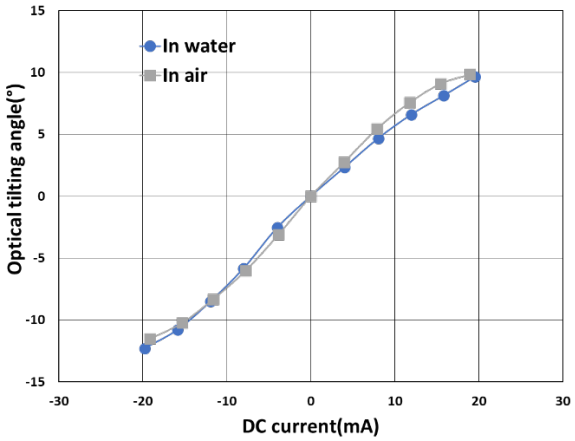

Fig. 6 The DC tilting angles of the slow axis in air and water for the scanning mirror.

Fig. 7 Representative laser scanning traces generated by the scanning mirror with the fast and slow axes driven at 206 Hz (fast) and DC (slow) in water.

5. Imaging Experiment

Pulse-echo ultrasound microscopy was conducted with the scanning mirror to demonstrate its underwater ultrasound beam steering capability. Fig. 8 shows the experimental setup of the ultrasound imaging test. The scanning mirror was held by a clamp at 45° facing down. A 25-MHz ultrasound transducer (with 31.75-mm focal length) was fixed horizontally

at a distance about 6 mm. A fiberglass window screen sheet was placed underneath of the scanning mirror at a distance about 25 mm, serving as the imaging target. The ultrasound signal transception of the transducer was controlled by a pulser/receiver. The pulser/receiver was triggered by a function generator at 12.36 kHz. The fast and slow axes of the scanning mirror were driven simultaneously by a two-channel function generator. A data acquisition (DAQ) card was used to record the ultrasound echo signals for image reconstruction. To synchronize the operation of the scanning mirror and the pulser/receiver, the function generator and the pulser/receiver were both triggered by the DAQ card. The fast axis of the scanning mirror was driven by an 8.5-mA AC current at 206 Hz. The slow axis was driven by a 10-mA (sinusoidal) AC current at 0.125 Hz. This creates a field view of 8.5 × 7.5 mm2 at a distance of 25 mm. Within each cycle of fast-axis scanning, there were 60 data points determined by the ratio between the ultrasound pulse repetition rate (12.36 kHz) and the frequency of the driving signal (206 Hz). Only 30 data points were utilized for the image reconstruction because of the two overlapped traces within each scanning cycle. For the slow-axis, it consists of 1648 scanning cycles of the fast-axis. Only 824 lines were utilized for the image reconstruction because of the two overlapped traces within each scanning cycle. As a result, a total number of 24720 (30 × 824) data points were used for the image reconstruction. The ultrasound image reconstruction followed a similar process previously reported [12]. Fig. 9 shows a representative B-mode image and the reconstructed overall 3D image in Volview®. From the reconstructed ultrasound image, the width and spacing of fiberglass threads are determined to be 400 um and 1.5 mm, respectively, which are close to the actual values. The edges of the ultrasound image do not appear as clear as the center region. This is because the fiberglass window sheet was placed on a flat surface, while the focal point of the ultrasound transducer was aligned to its center region. When the mirror plate is tilted to a larger angle, the work distance between the target and the ultrasound transducer will change, which could make the target out of focus. This issue can be addressed by fixing the fiberglass window screen onto a concave surface to make all the scan points remain inside the focal zone.

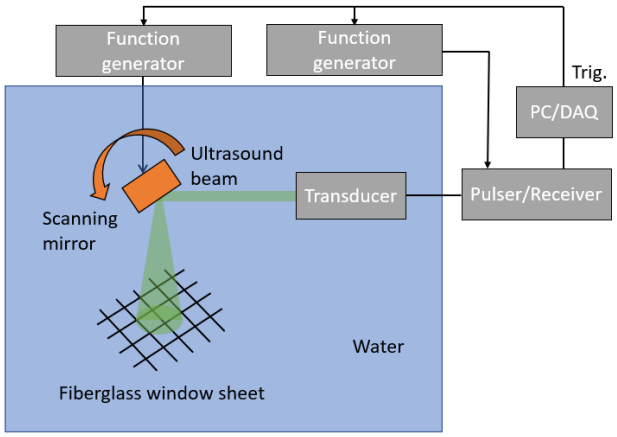

Fig. 8 Schematic of the pulse-echo ultrasound microscopy setup.

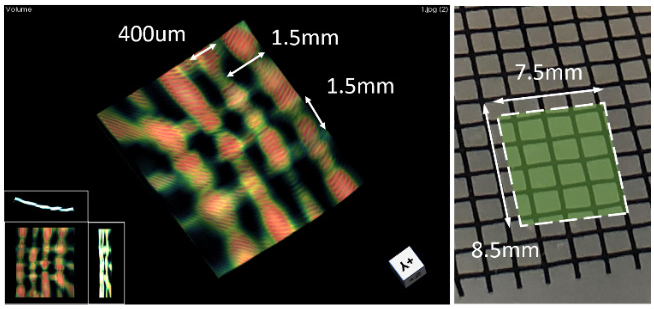

Fig. 9 Reconstructed (a) B-mode and (b) 3D image of a fiberglass window screen sheet.

6. CONCLUSION

In summary, a new micromachined water-immersible micro scanning mirror with a hybrid torsional and bending polymer hinge structure has been has been demonstrated. The combination of the torsional and bending modes makes it possible to achieve very different driving frequencies of the fast and slow axes with single hinge material. Such feature is especially useful for generating a dense raster scanning pattern for scanning optical and acoustic microscopy. For demonstration, scanning ultrasound microscopy has also been conducted with the hybrid-hinge scanning mirror. In the future, the mirror packaging will be optimized to minimize the shift of the resonance frequencies caused by the amplitude-dependent viscous damping.

ACKNOWLEDGMENTS

This work was supported in part by awards (NRI-1925037 and CBET-2036134) from the National Science Foundation and a grant (1R01NS115581-01) from the National Institutes of Health to JZ.

REFERENCES

[1] D. Wang, L. Thomas, S. Koppal, Y. Ding and H. Xie, "A Low-Voltage, Low-Current, Digital-Driven MEMS Mirror for Low-Power LiDAR," in IEEE Sensors Letters, vol. 4, no. 8, pp. 1-4, Aug. 2020, Art no. 5000604, doi: 10.1109/LSENS.2020.3006813.

[2] D. Wang, S. J. Koppal and H. Xie, "A Monolithic Forward-View MEMS Laser Scanner With Decoupled Raster Scanning and Enlarged Scanning Angle for Micro LiDAR Applications," in Journal of Microelectromechanical Systems, vol. 29, no. 5, pp. 996-1001, Oct. 2020, doi: 10.1109/JMEMS.2020.3001921.

[3] K. H. Koh, Y. Qian and C. Lee, "Design and characterization of a 3D MEMS VOA driven by hybrid electromagnetic and electrothermal actuation mechanisms," in J. Micromech. Microeng., vol. 22, no. 10, pp. 1- 13, 2012, doi: 10.1088/0960-1317/22/10/105031.

[4] H. Yang, D. Wang, T. Shan, X. Dai, H. Xie, L. Yang, H. Jiang, "Miniature fluorescence molecular tomography (FMT) endoscope based on a MEMS scanning mirror and an optical fiberscope," in Phys Med Biol. Jun. 2019, 64(12):125015, doi: 10.1088/1361-6560/ab23b3.

[5] S. Luo, D. Wang, J. Tang, L. Zhou, C. Duan, D. Wang, H. Liu, Y. Zhu, G. Li, H. Zhao, Y. Wu, X. An, X. Li, Y. Liu, L. Huo, and H. Xie, "Circumferential-scanning endoscopic optical coherence tomography probe based on a circular array of six 2-axis MEMS mirrors," in Biomed. Opt. Express, vol. 9, pp. 2104-2114, 2018, doi: 10.1364/BOE.9.002104.

[6] C. H. Huang, J. Yao, L. V. Wang, and J. Zou, "A water-immersible 2-axis scanning mirror microsystem for ultrasound and photoacoustic microscopic imaging applications," in Microsystem technologies, 19(4), pp. 577-582, 2013, doi: 10.1007/s00542-012-1660-4.

[7] J. Y. Kim, C. Lee, K. Park, G. Lim, and C. Kim, "Fast optical-resolution photoacoustic microscopy using a 2-axis water-proofing MEMS scanner," in Scientific Reports, 5(1), 7932, 2015, doi: 10.1038/srep07932.

[8] S. Xu, and J. Zou, "Two-axis water-immersible micro scanning mirror for scanning optics and acoustic microscopy," in SPIE Journal of Micro/Nanolithography, MEMS, and MOEMS, 15(4), 045005, 2016, doi: 10.1117/1.JMM.15.4.045005.

[9] S. Xu, X. Duan, and J. Zou, "A Two-Axis Water-Immersible Micro Scanning Mirror Driven by Single Inductor Coil through Dynamic Structural Filtering," in Sensors and Actuators A: Physical, 284(12), pp. 172-180, 2018, doi: 10.1016/j.sna.2018.10.029.

[10] S. Xu, S. Li, and J. Zou, "A micromachined water-immersible scanning mirror using BoPET hinges," in Sensors and Actuators A: Physical, 298, 111564, 2019, doi: 10.1016/j.sna.2019.111564.

[11] X. Duan, S. Li, A. Medellin, C. Ma, and J. Zou, "A two-axis water-immersible micro scanning mirror using hybrid polymer and elastomer hinges," in Sensors and Actuators A: Physical, 312, 112108, 2020, doi: 10.1016/j.sna.2020.112108.

[12] P. E. Dyer, G. A. Oldershaw, and J. Sidhu, “CO2 laser ablative etching of polyethylene terephthalate,” in Applied Physics B, 48(6) pp. 489-493, 1989, doi: 10.1007/BF00694685.